
**Separation Science and Technology**
Publication details, including instructions for authors and subscription information:
http://www.informaworld.com/smpp/title~content=t713708471

# Soil Clean Up by *in-situ* Aeration. IV. Anisotropic Permeabilities

Robert D. Mutch Jr.[a]; David J. Wilson[b]
[a] ECKENFELDER, Inc., MAHWAH, NEW JERSEY [b] DEPARTMENTS OF CHEMISTRY AND OF CIVIL AND ENVIRONMENTAL ENGINEERING, VANDERBILT UNIVERSITY, NASHVILLE, TENNESSEE

**To cite this Article** Mutch Jr., Robert D. and Wilson, David J.(1990) 'Soil Clean Up by *in-situ* Aeration. IV. Anisotropic Permeabilities', Separation Science and Technology, 25: 1, 1 — 29
**To link to this Article: DOI:** 10.1080/01496399008050318
**URL:** http://dx.doi.org/10.1080/01496399008050318

SEPARATION SCIENCE AND TECHNOLOGY, 25(1 & 2), pp. 1-29, 1990

# Soil Clean Up by *in-situ* Aeration. IV. Anisotropic Permeabilities

ROBERT D. MUTCH JR.

ECKENFELDER, Inc.*
MAHWAH, NEW JERSEY 07430

DAVID J. WILSON†

DEPARTMENTS OF CHEMISTRY AND OF CIVIL AND ENVIRONMENTAL ENGINEERING
VANDERBILT UNIVERSITY
NASHVILLE, TENNESSEE 37235



**Abstract**

A method for determining the ratio of the vertical and horizontal permeabilities of soils to air is described. The method requires measurement of the gas flow rate in a vacuum well and the soil gas pressure at a suitably chosen point in the vicinity of the well. Soil gas pressures in the vicinity of a vaccum well in an anisotropic medium are calculated theoretically by using the method of images to construct a solution to Laplace's equation which satisfies the appropriate boundary conditions. Effects of well depth, depth of water table, and anisotropy are examined. A relaxation method is presented for determining soil gas pressure distributions when the permeability is both anisotropic and a function of position. It is shown that piezometer measurements in the vicinity of a vacuum well permit the location of strata of differing permeabilities.

*Formerly AWARE, Inc.
†To whom correspondence should be addressed.

## INTRODUCTION

The U.S. Environmental Protection Agency now has over 1200 sites on its National Priority (Superfund) List; in addition, it is estimated that several thousand other sites will require clean up if contamination of groundwater with toxic chemicals is to be avoided or remediated. A very substantial number of these sites are contaminated with volatile hydrophobic organics (gasoline, chlorinated solvents, toluene, xylenes, etc.) which, as Schwille (*1*) has noted, move quite rapidly in both the vadose zone and the zone of saturation. These materials are amenable to removal by *in-situ* soil vapor stripping, the advantages of which were described in our earlier papers (*2–4*). The technique is now coming into relatively common use, and a substantial literature on soil vapor stripping is developing.



Laboratory-scale investigations include Wootan and Voynick's work on vapor stripping gasoline from a large-scale sand aquifer (*5*) and Clarke's work on vapor stripping of several volatile organic compounds in laboratory columns (*6*). A pilot-scale vapor stripping operation near Tacoma, Washington, was described by Woodward-Clyde Consultants (*7*), and Anastos et al. (*8*) discussed a pilot study of the removal of trichloroethylene and other volatiles at the Twin Cities Army Ammunition Plant, Minnesota. Crow, Anderson, and Minugh (*9*) reported on soil vapor stripping at a petroleum fuels terminal, and Bailey and Gervin (*10*) described a pilot study of vapor stripping of chlorinated solvents. Lord (*11*) successfully vapor stripped gasoline in the vicinity of streets and buildings, and recently Terra Vac (*12*) carried out a demonstration test at Groveland, Massachusetts.

Previously we presented mathematical models for simulating lab column and field-scale vapor stripping, and we discussed the use of lab column data with the lab column model to obtain parameters for the field-scale model. The effects of well depth, well packing radius, impermeable overlying caps, impermeable obstacles in the soil, evaporative cooling, passive vent wells, and the removal of underlying nonaqueous phase liquid (NAPL) by vapor stripping were examined (*2–4, 13, 14*).

In most of our previous work it was assumed that the permeability of the soil being vapor stripped is isotropic. It was noted that anisotropic permeabilities could be handled by transforming to the principal axes of the permeability tensor and making suitable scale changes, but all of our computations were carried out on isotropic systems. It is well known that permeabilities of rocks, sands, and clays to water are not isotropic; horizontal components of the permeability are often several times larger

than the vertical component (*15*). It therefore seems quite reasonable that the permeabilities to air of geological media in the vadose zone might be anisotropic, too. This should result in changes in the flow patterns of the soil gas as it moves toward the stripping well; these changes, in turn, should cause changes in the optimal design of vapor stripping well arrays. If, for instance, the horizontal permeability is substantially greater than the vertical permeability, one should be able to space the vacuum wells farther apart, with a corresponding reduction in cost.

In the present paper we address the problem of calculating the soil gas pressure distribution in the vicinity of a single vacuum well screened at an arbitary distance above the water table; this is done by the method of images. This solution is then used to explore the effects of well depth, depth of water table, and soil anisotropy on the soil gas pressures at various points in the zone of influence of the vacuum well. These pressures are readily measured by piezometer wells. The results permit one to optimize the location of piezometer wells to measure the soil anisotropy with maximum sensitivity. A relaxation method is developed for calculating soil gas pressures around a vacuum well in a medium having a permeability which is both anisotropic and variable from point to point. The effect of strata of differing permeabilites on the soil gas pressure distribution is then explored.



## ANALYSIS, ANISOTROPIC, CONSTANT PERMEABILITY

In the first paper in this series it was shown that the square of the soil gas pressure in the vicinity of a vapor stripping well obeys Laplace's equation, and that, if the porous medium has an anisotropic permeability, the square of the pressure obeys

$$\nabla \cdot K \nabla P^2 = 0 \tag{1}$$

where $K$ is the permeability tensor. If our system may be adequately approximated as having cylindrical symmetry, then the permeability tensor is

$$K = \begin{pmatrix} K_r & 0 \\ 0 & K_z \end{pmatrix}$$

In cylindrical coordinates with the assumption of cylindrical symmetry

(with the vapor stripping well located on the $z$ axis of the coordinate system), Eq. (1) becomes

$$\frac{1}{r}\frac{\partial}{\partial r}\left(r\frac{\partial U}{\partial r}\right)+\frac{\alpha^2\partial^2 U}{\partial z^2}=0 \tag{2}$$

where $\alpha^2 = K_z/K_r$.

We assume a trial solution for Eq. (2),

$$U=\frac{1}{(r^2+\beta^2 z^2)^{1/2}} \tag{3}$$

On substitution of Eq. (3) into Eq. (2), we find that $U$ is a solution if $\beta = \alpha^{-1}$, so

$$U=\frac{A}{(r^2+z^2/\alpha^2)^{1/2}} \tag{4}$$

is a solution. A more general solution is obtained by transforming the origin along the $z$ axis; it is

$$U=\frac{A}{\{r^2+[(z-a)/\alpha]^2\}^{1/2}} \tag{5}$$

A still more general solution is a linear combination of terms of the type given in Eq. (5),

$$U=\sum_i \frac{A_i}{\{r^2+[(z-a_i)/\alpha]^2\}^{1/2}} \tag{6}$$

This result indicates that we can, as in the isotropic case, use the method of images from electrostatics to construct solutions of Eq. (2) satisfying the desired boundary conditions.

We let the first term in the above solution represent the actual sink (the vacuum well), located at $(0,a_1)$. The constant $A_1$ in this term is evaluated as follows. Recall that, since the soil gas is assumed to be ideal,

$$P^2 = U + \text{constant} \tag{7}$$

Let $Q$ be the magnitude of the molar gas flow rate at the sink. Then

$$Q = -\int_0^{2\pi}\int_{-\infty}^{\infty} \nu c \mathbf{v} \cdot d\mathbf{S} \tag{8}$$

Here the surface $S$ is taken to be an infinitely long cylinder of radius $r'$ coaxial with the $z$ axis.

Let $\nu$ = voids fraction of the soil
$c$ = concentration of gas, mol/m$^3$
$v$ = linear velocity of the gas at the surface over which the integral is taken
$c$ = $P/RT$
$R$ = $8.206 \times 10^{-5}$ m$^3 \cdot$ atm/mol $\cdot$ degree

Then

$$Q = \frac{\nu}{RT}\int_0^{2\pi}\int_{-\infty}^{\infty} PK_r \frac{\partial P}{\partial r} r' d\theta dz \tag{9}$$

$$= \frac{\nu K_r 2\pi r'}{RT}\int_{-\infty}^{\infty} \frac{1}{2} \frac{\partial (P^2)}{\partial r} dz \tag{10}$$

We are concerned only with the sink at $(0,a_1)$, so we take

$$P^2 = 1 \text{ atm}^2 - \frac{A_1}{\{r^2 + [(z - a_1)/\alpha]^2\}^{1/2}} \tag{11}$$

[dropping those terms which do not represent a source at $(0,a_1)$]. Then

$$\frac{\partial P^2}{\partial r} \approx \frac{A_1 r}{\{r^2 + [(z - a_1)/\alpha]^2\}^{3/2}} \tag{12}$$

and

$$Q = \frac{\pi \nu K_r (r')^2 A}{RT}\int_{-\infty}^{\infty} \frac{dz'}{[(r')^2 + (z'/\alpha)^2]^{3/2}} \tag{13}$$

$$z' = z - a_1$$

$$Q = \frac{2\pi K_r \nu A_1}{RT} \int_{-\infty}^{\infty} \frac{(r')^2}{(r')^3} \frac{dz'}{[1 + (z'/r'\alpha)^2]^{3/2}} \tag{14}$$

Let $\xi = z'/(r'\alpha)$; $dz' = \alpha r' d\xi$. Then

$$Q = \frac{2\pi \nu K_r A_1 \alpha}{RT} \int_{-\infty}^{\infty} \frac{d\xi}{(1 + \xi^2)^{3/2}} \tag{15}$$

The definite integral in Eq. (15) is equal to 1 (*17*). So

$$Q = \frac{2\pi \nu K_r A_1 \alpha}{RT} \tag{16}$$

and

$$A_1 = \frac{RTQ}{2\pi \nu \alpha} \tag{17}$$

and, on substituting for $\alpha$,

$$A_1 = \frac{RTQ}{2\pi \nu (K_r K_z)^{1/2}} \tag{18}$$

Then we can write

$$P^2 = W - \frac{RTQ}{2\pi \nu (K_r K_z)^{1/2}} \frac{1}{\{r^2 + [z - a_1)/\alpha]^2\}^{1/2}} \tag{19}$$

where $W$ is a solution of Eq. (2) which is regular at $(0,a_1)$. This could be used as a starting point for a numerical relaxation approach. We employ instead the method of images.

The geometry of our system is shown in Fig. 1. The boundary conditions appropriate to this system are

$$P^2 - 1 = 0 \text{ at } (r,b) \tag{20}$$

since the pressure must be 1 atmosphere at the surface of the soil, and

$$\partial P^2/\partial z = 0 \text{ at } (r_0)$$

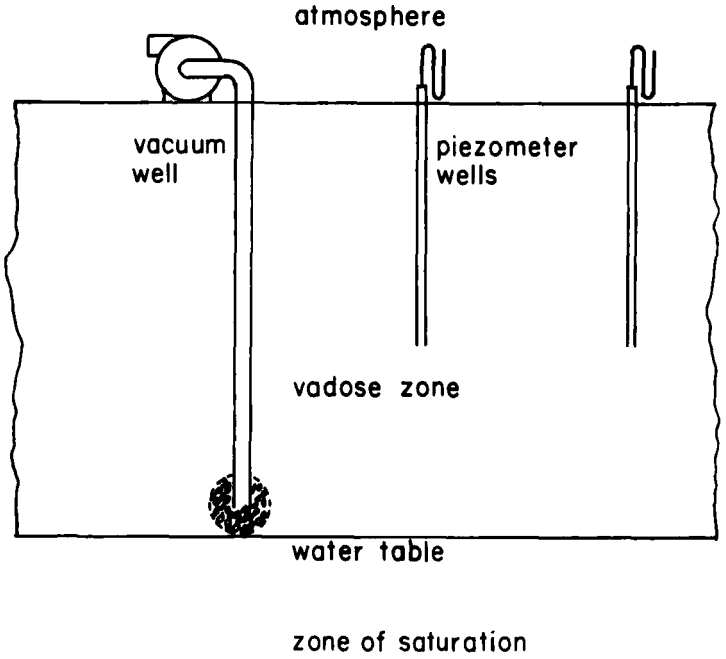


FIG. 1. Model of a vacuum well and piezometer wells for measuring soil permeability and its anisotropy.



since there can be no gas flow normal to the water table at the bottom of the vadose zone. We henceforth drop the subscript from $a_1$, so that the sink is located at $(0,a)$. The location of the sink, together with Eqs. (20) and (21) and the requirement that our solution be of the form given by Eq. (6), gives us the following series solution for $P^2(r,z)$:

$$P^2(r,z) = 1 + \sum_{i=1}^{\infty} \frac{A_i}{\{r^2 + [(z - a_i)/\alpha]^2\}^{1/2}} \tag{22}$$

where the first 22 values of the $A_i$ and $a_i$ are given in Table 1. To adjust (approximately) for the fact that we are not taking the full infinite series, we let

$$C = - \sum_{i=1}^{22} \frac{A_i}{\{0^2 + [(b - a_i)/\alpha]^2\}^{1/2}} \tag{23}$$

TABLE 1

| | Image potential | Parameter values |
|---|---|---|
| $i$ | $a_i$ | $A_i$ |
| 1 | $a$ | $-A$ |
| 2 | $-a$ | $-A$ |
| 3 | $2b + a$ | $A$ |
| 4 | $2b - a$ | $A$ |
| 5 | $-2b + a$ | $A$ |
| 6 | $-2b - a$ | $A$ |
| 7 | $4b + a$ | $-A$ |
| 8 | $4b - a$ | $-A$ |
| 9 | $-4b + a$ | $-A$ |
| 10 | $-4b - a$ | $-A$ |
| 11 | $6b + a$ | $A$ |
| 12 | $6b - a$ | $A$ |
| 13 | $-6b + a$ | $A$ |
| 14 | $-6b - a$ | $A$ |
| 15 | $8b + a$ | $-A$ |
| 16 | $8b - a$ | $-A$ |
| 17 | $-8b + a$ | $-A$ |
| 18 | $-8b - a$ | $-A$ |
| 19 | $10b - a$ | $A$ |
| 20 | $10b + a$ | $A$ |
| 21 | $-10b + a$ | $A$ |
| 22 | $-10b - a$ | $A$ |



and write

$$P^2(r,z) = 1 + C + \sum_{i=1}^{22} \frac{A_i}{\{r^2 + [(z - a_i)/\alpha]^2\}^{1/2}} \tag{24}$$

Then

$$P(r,z) = (P^2)^{1/2} \tag{25}$$

Generally, one can measure the molar gas flow rate and the gas pressure at the well head, $P_f$ ($< 1$ atm). From this we can calculate $(K_rK_z)^{1/2}$ as follows.

$$P_f^2 = 1 - \frac{RTQ}{2\pi v(K_r K_z)^{1/2}} \frac{1}{(r_s^2)^{1/2}} \tag{26}$$

from which we readily obtain

$$(K_r K_z)^{1/2} = \frac{RTQ}{2\pi v r_s (1 - P_f^2)} \tag{27}$$

A computer program was written in BASICA implementing this model; this yielded the results described in the next section.

## RESULTS, METHOD OF IMAGES



A list of the standard parameter set generally used is given in Table 2. Parameters not listed there and departures from those values are given in the captions to the figures.

The ability of the image solution to fit the boundary condition that $P^2 = 1$ at the surface of the soil is illustrated in Table 3; the errors are of the order of a thousandth of an inch of water or less, and are negligible to all intents and purposes.

The effect of the depth of the vacuum well on soil gas pressure is shown in Fig. 2 for piezometer wells screened at a depth of 4 m and located at distances of 0, 2, 5, and 10 m from the vacuum well. One wishes to avoid vacuum well–piezometer well configurations in which the soil gas pressure varies rapidly with the position of the piezometer well; one also wishes to have the soil gas pressure (actually measured in inches of water

TABLE 2
The Standard Parameter Set

| | |
|---|---|
| Water table depth | 12 m |
| Piezometer well depth | 4 m |
| Vacuum well molar flow rate | 0.1 mol/s |
| Screened radius of vacuum well | 0.12 m |
| Soils voids fraction | 0.2 |
| Pressure at head of vacuum well | 0.866 atm |
| Temperature | 12°C |
| $K_r/K_z$ | 1 |
| $K_r$ | 0.06228 $m^2$/atm · s |

TABLE 3
Test of 1 atm Boundary Condition at Soil Surface

| | |
|---|---|
| Run conditions: | |
| Depth of water table | 20 m |
| Depth of vacuum well | 18 m |
| Vacuum well molar flow rate | 0.6 mol/s |
| $K_z/K_r$ | 1 |
| $K_r$ | 0.1861738 $m^2/atm \cdot s$ |
| $r$ (m) | Calculated vacuum at soil surface, in $H_2O$ |
| 30 | −0.00082 |
| 25 | −0.00060 |
| 20 | −0.00037 |
| 15 | −0.00018 |
| 10 | −0.00009 |
| 5 | 0.00000 |
| 0 | 0.00002 |



vacuum) sufficiently large to permit its measurement with reasonably high percentage accuracy. Of the well configurations described in Fig. 2, a vacuum well depth of at least 4 m and a distance between the vacuum well and the piezometer well of about 5 m would apppear to be fairly satisfactory. If the vacuum well is at least 8 m deep, then one could place the piezometer well substantially closer to the vacuum well and still not have strong dependence of the soil gas pressure on the precise location of the piezometer.

We had originally hoped that the location of the water table with respect to the vacuum well would be relatively unimportant. In Fig. 3 we see that the piezometer pressures depend significantly on the depth of the water table up to depths which are roughly double the depth of the vacuum well, so that accurate knowledge of the depth of the water table and the depth of the vacuum well is necessary to interpret piezometer readings accurately in terms of soil permeability. In our earlier work we concluded that vapor stripping wells are most efficient if they are drilled down quite close to the water table. Our results here suggest that vacuum wells drilled for measuring soil permeabilities might give more accurate results if they are not drilled down almost to the water table, since under these circumstances a relatively small change in the well depth can result in a rather substantial change in piezometer reading.

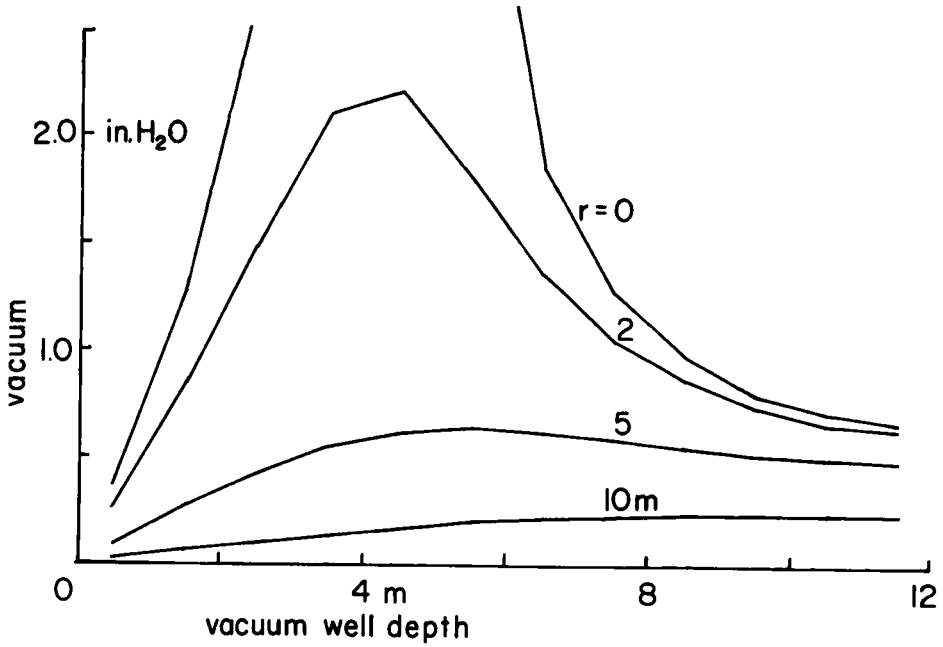


FIG. 2. Effect of vacuum well depth on piezometer readings at constant water table depth. Distance $r$ between well and piezometer well = 0, 2, 5, and 10 m as indicated; other parameters are in Table 2. All piezometer readings in the figures are in inches of water vacuum.



Figures 4 and 5 show the dependence of piezometer readings on the anisotropy of the soil permeability. In both figures the depth of the piezometers is 4 m; the depth of the water table in Fig. 4 is 50 m, while it is only 12 m in Fig. 5. We note that the pressure plots are double-valued functions of the anisotropy ratio $K_z/K_r$ for piezometers located at a distance of 10 m from the vacuum well, and that these plots are also rather flat. Evidently one could obtain more accurate values of the anisotropy ratio by locating piezometers at a distance of from 2 to 5 m from the vacuum well. (A location immediately adjacent to the vacuum well looks attractive from the figures, but this soil may be significantly disturbed by the drilling of the vacuum well.) The very marked difference in the dependence of the soil gas pressure on the anisotropy ratio for piezometers located 2–5 m from the vacuum well and located 20 m from the vacuum well can be used to test the applicability of this model in a given situation. (Piezometer

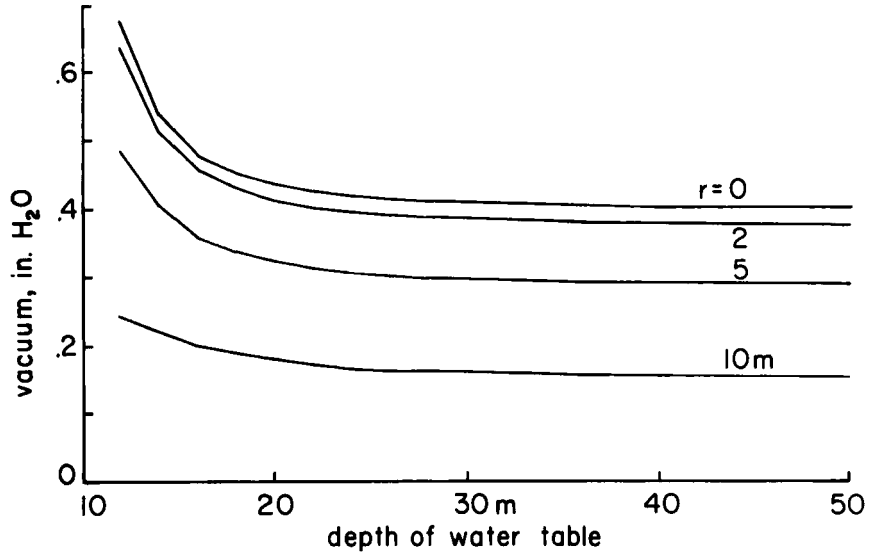


FIG. 3. Effect of water table depth of piezometer readings. $r$ = 0, 2, 5, and 10 m as indicated; vacuum well depth = 11.5 m; other parameters as in Table 2.



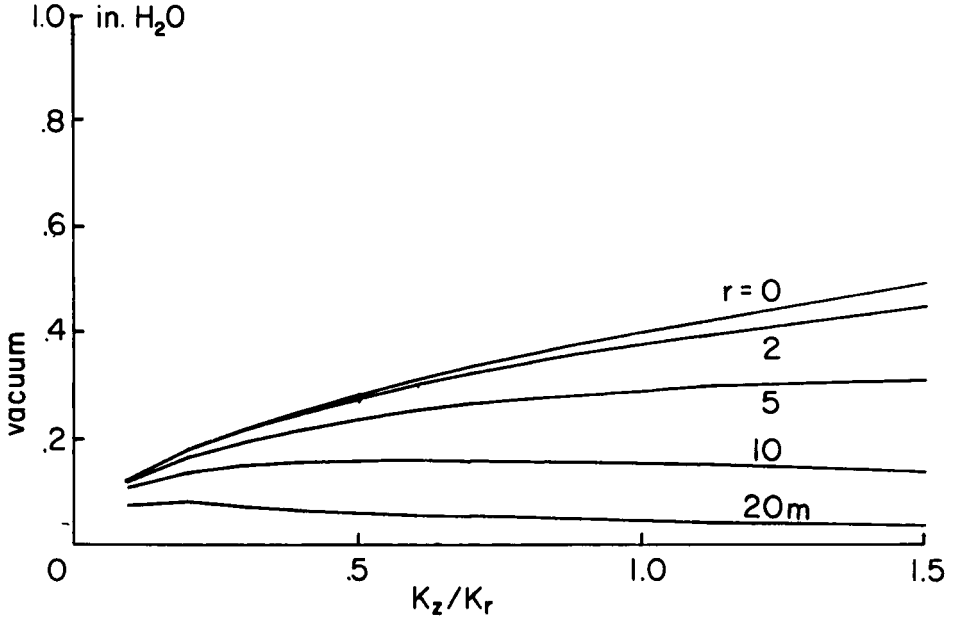


FIG. 4. Effect of permeability anisotropy $K_z/K_r$ on piezometer readings with a water table depth of 50 m. Depth of vacuum well = 11.5 m; $r$ = 0, 2, 5, 10, and 20 m as indicated. Other parameter as in Table 2.

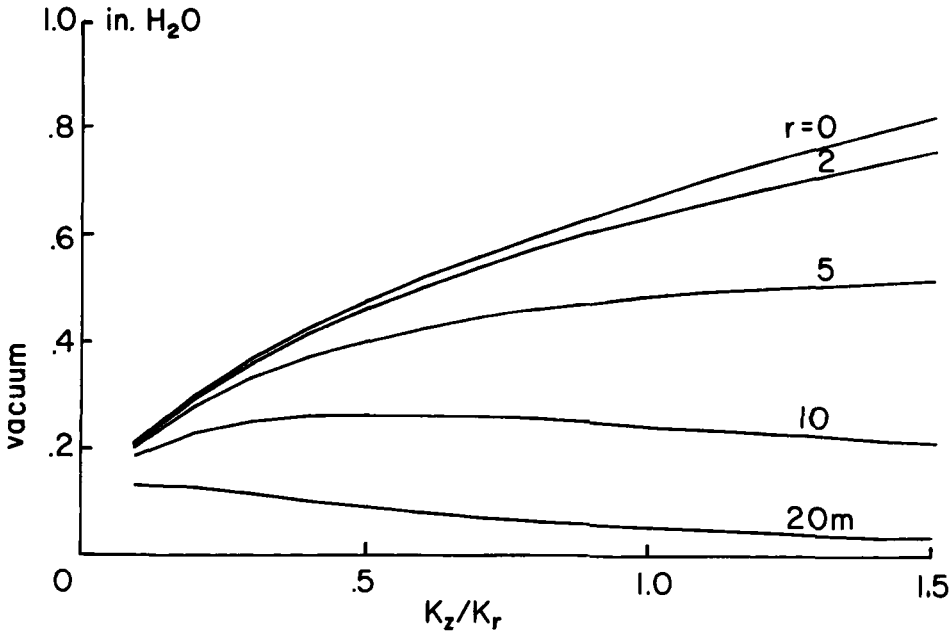


FIG. 5. Effects of permeability anisotropy $K_z/K_r$ on piezometer readings with a water table depth of 12 m. Depth of vacuum well = 11.5 m; $r$ = 0, 2, 5, 10, and 20 m as indicated. Other parameters as in Table 2.



readings increase with increasing anisotropy ratio near the vacuum well, but decrease with increasing anisotropy ratio at distances much greater than 10 m.)

These results indicate that the anisotropy of soil permeability to air can be measured by determining the gas flow rate through a vacuum well operating at a given vacuum and by determining the soil gas pressure at one or more suitably located piezometers in the vicinity of the vacuum well. Such results would be useful in determining the applicability of models which assume that the soil permeability to air is isotropic, and the pressure distributions obtained can then be used in calculating soil gas velocities in anisotropic media for use in a model for field vapor stripping well operation.

## VARIABLE PERMEABILITY

If the permeability of the soil to air is not only anisotropic but varies from point to point in the domain of interest, one can apparently not use

the method of images to calculate the velocity potential, $P^2$. A typical situation might be that a rather permeable sandy soil is overlain with a layer of less permeable clay. We shall assume that the problem has axial symmetry, so that Eq. (1) becomes

$$\frac{1}{r}\frac{\partial}{\partial r}\left(rK_r\frac{\partial P^2}{\partial r}\right) + \frac{\partial}{\partial z}\left(K_z\frac{\partial P^2}{\partial z}\right) \tag{28}$$

We also assume that $K_r = K_r(z)$ and $K_z = K_z(z)$—that the components of the permeability depend on depth alone over the domain of interest.

The numerical integration of Eq. (28) is done as follows. The cylindrical domain of interest is partitioned into ring-shaped volume elements as indicated in Fig. 6. For the $ij$th volume element,

$$r_i = (i + 1/2)\Delta r$$

$$\text{inner surface} = 2\pi i\Delta r\Delta z$$

$$\text{outer surface} = 2\pi(i + 1)\Delta r\Delta z$$

$$\text{upper and lower surfaces} = \pi(2i + 1)\Delta r^2$$



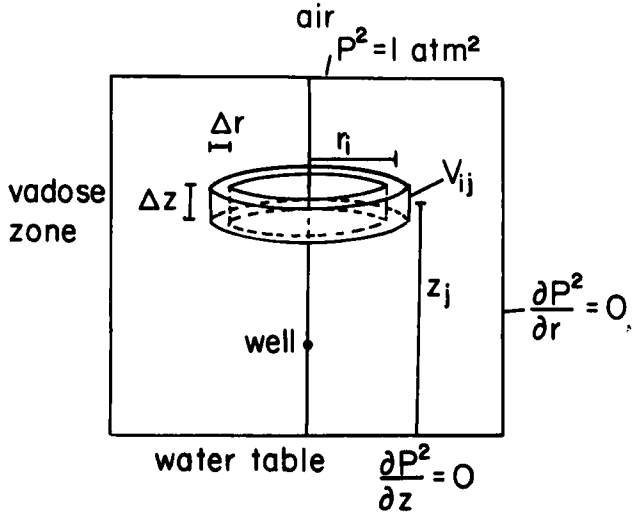


FIG. 6. Geometry, notation, and boundary conditions for a vapor stripping well. Partitioning of the domain of interest.

We next calculate the net flux into the $ij$th volume element, as in electrostatics or diffusion calculations. The ranges of the indices are $i = 0, 1, 2, \ldots, n_r$; $j = 0, 1, 2, \ldots, n_z$.

$$\begin{aligned}\text{Net flux} = 0 = {} & K_r[(j + \tfrac{1}{2})\Delta z]2\pi i\Delta r\Delta z(P^2_{i-1,j} - P^2_{i,j}) \\ & + K_r[(j + \tfrac{1}{2})\Delta z]2\pi(i + 1)\Delta r\Delta z(P^2_{i+1,j} - P^2_{i,j}) \\ & + K_z[j\Delta z]\pi(2i + 1)\Delta r^2(P^2_{i,j-1} - P^2_{i,j}) \\ & + K_z[(j + 1)\Delta z]\pi(2i + 1)\Delta r^2(P^2_{i,j+1} - P^2_{i,j}) \end{aligned} \tag{29}$$

We solve Eq. (29) for $P^2_{i,j}$ after setting $\Delta r = \Delta z = \delta$.

$$P^2_{i,j} = \frac{\begin{aligned}&\{2iK_r[(j + \tfrac{1}{2})\delta]P^2_{i-1,j} + 2(i + 1)K_r[(j + \tfrac{1}{2})\delta]P^2_{i+1,j} \\ &+ (2i + 1)K_z(j\delta)P^2_{i,j-1} + (2i + 1)K_z[(j + 1)\delta]P^2_{i,j+1}\}\end{aligned}}{(4i + 2)K_r[(j + \tfrac{1}{2})\delta] + (2i + 1)[K_z[j\delta] + K_z[(j + 1)\delta]]} \tag{30}$$

Our boundary conditions are

$$P^2 = 1 \text{ atm}^2 \tag{31}$$

on the top of the zone of influence,

$$\partial P^2/\partial r = 0 \tag{32}$$

around the periphery of the zone of influence, and

$$\partial P^2/\partial z = 0 \tag{33}$$

on the base of the zone of influence. We carry out flux balances on each of the volume elements on the surface of the domain of interest which are consistent with boundary conditions, with the following results.

At the top of the boundary, where $P^2 = 1$:

$$\begin{aligned}0 = {} & K_r[(n_z + \tfrac{1}{2})\Delta z]2\pi i(P^2_{i-1,nz} - P^2_{i,nz}) \\ & + K_r[(n_z + \tfrac{1}{2})\Delta z]2\pi i(i + 1)(P^2_{i+1,nz} - P^2_{i,nz}) \\ & + K_z[j\Delta z]\pi(2i + 1)(P^2_{i,nz-1} - P^2_{i,nz}) \\ & + 2K_z[(j + 1)\Delta z]\pi(2i + 1)(1 - P^2_{i,nz}) \end{aligned} \tag{34}$$

Along the outer boundary, where $\partial P^2/\partial r = 0$:

$$0 = K_r[(j + \tfrac{1}{2})\Delta z]2\pi i n_r(P^2_{nr-i,j} - P^2_{nr,j}) + K_z[(j\Delta z]\pi(2n_r + 1)(P^2_{nr,j-1} - P^2_{nr,j}) + K_z[j + 1)\Delta z]\pi(2n_r + 1)(P^2_{nr,j+1} - P^2_{nr,j}) \quad (35)$$

Along the bottom boundary, where $\partial P^2/\partial z = 0$:

$$0 = K_r[\tfrac{1}{2}\Delta z]2\pi i(P^2_{i-1,0} - P^2_{i,0}) + K_r[\tfrac{1}{2}z]2\pi(i + 1)(P^2_{i+1,0} - P^2_{i,0}) + K_z[\Delta z]\pi(2i + 1)(P^2_{i,1} - P^2_{i,0}) \quad (36)$$

Along the left boundary (the axis of the domain) we can use Eq. (29), since the coefficient of the term in $P^2_{i-1,j}$ vanishes when $i = 0$. In upper left corner (on the axis):

$$0 = K_r[(n_z + \tfrac{1}{2})\Delta z]2\pi(P^2_{1,nz} - P^2_{0,nz}) + K_z[(n_z\Delta z]\pi(P^2_{0,nz-1} - P^2_{0,nz}) + 2K_z[(n_z + 1)\Delta z]\pi(1 - P^2_{0,nz}) \quad (37)$$

In the upper right corner:

$$0 = K_r[(n_z + \tfrac{1}{2})\Delta z]2\pi n_r(P^2_{nr-1,nz} - P^2_{nr,nz}) + K_z[n_z\Delta z]\pi(2n_r + 1)\pi(n_r + 1)(P^2_{nr,nz-1} - P^2_{nr,nz}) + 2K_z[(n_z + 1)\Delta z]\pi(2n_r + 1)(1 - P^2_{nr,nz}) \quad (38)$$

In the lower left corner:

$$0 = K_r[\tfrac{1}{2}\Delta z]2\pi(P^2_{1,0} - P^2_{0,0}) + K_z[\Delta z]\pi(P^2_{0,1} - P^2_{0,0}) \quad (39)$$

And in the lower right corner:

$$0 = K_r[\tfrac{1}{2}\Delta z]2n_r\pi(P^2_{nr-1,0} - P^2_{nr,0}) + K_z[\Delta z](2n_r + 1)\pi(P^2_{nr,1} - P^2_{nr,0}) \quad (40)$$

Equations (34)–(40) are solved for the central value of $P^2$, as was done in obtaining Eq. (30) from Eq. (29). The results, along with Eq. (30), are the relaxation equations.

The effective pressure in the volume element surrounding the sink (the well) is estimated as follows. Recall that in the vicinity of the well,

$$P^2 \approx 1 \text{ atm}^2 - \frac{RTQ}{2\pi v(K_r K_z)^{1/2}} \frac{1}{\{r^2 + [(z - a)/\alpha]^2\}^{1/2}} \tag{41}$$

At the screened radius of the well we take

$$P_f^2 = 1 \text{ atm}^2 - \frac{RTQ}{2\pi v(K_r K_z)^{1/2} r_s} \tag{42}$$

where $P_f$ is the well head pressure and $r_s$ is the screened radius of the well. At the boundary of the volume element enclosing the sink,

$$\frac{1}{\{r^2 + [(z - a)/\alpha]^2\}^{1/2}} \approx \frac{1}{\delta} \tag{43}$$

At this surface $P_f'$, the mean effective pressure in this volume element, is therefore given by

$$(P_f')^2 = 1 \text{ atm}^2 - \frac{RTQ}{2\pi v(K_r K_z)^{1/2} \delta} \tag{44}$$

From Eq. (42),

$$\frac{RTQ}{2\pi v(K_r K_z)^{1/2}} = (1 - P_f^2) r_s \tag{45}$$

which we substitute into Eq. (44) to obtain

$$(P_f')^2 = 1 \text{ atm}^2 = 1 \text{ atm}^2 - (1 - P_f^2) \frac{r_s}{\delta} f \tag{46}$$

Here $f$ is a factor of the order of unity which is adjusted to give optimal agreement between the results of this method and the results of the method of images; a value of 2.04 is used in the following calculations.

We then include the boundary condition associated with the vacuum well by requiring that

$$P_{0,J}^2 = (P_f')^2 \tag{47}$$

where the sink is located in the (0,$J$)th volume element.

The molar flow rate $Q$ is related to the permeability components in the immediate vicinity of the well by Eq. (42), which gives

$$Q = (1 \text{ atm}^2 - P_f^2) \frac{2\pi\nu(K_r K_z)^{1/2} r_s}{RT} \tag{48}$$

## RESULTS, VARIABLE PERMEABILITY

A set of five runs was made for a configuration having the geometry shown in Fig. 7. The parameter used in these runs are given in Table 4. The objective was to determine the effect of strata of differing permeabilities on the soil gas pressure distribution. In Runs 1 and 2 the permeability of the overlying layer is greater than that of the lower layer. In Run 3 the permeabilities are identical. In Runs 4 and 5 the permeability of the overlying layer is less than that of the lower layer. In all cases it is assumed that the permeability is isotropic.



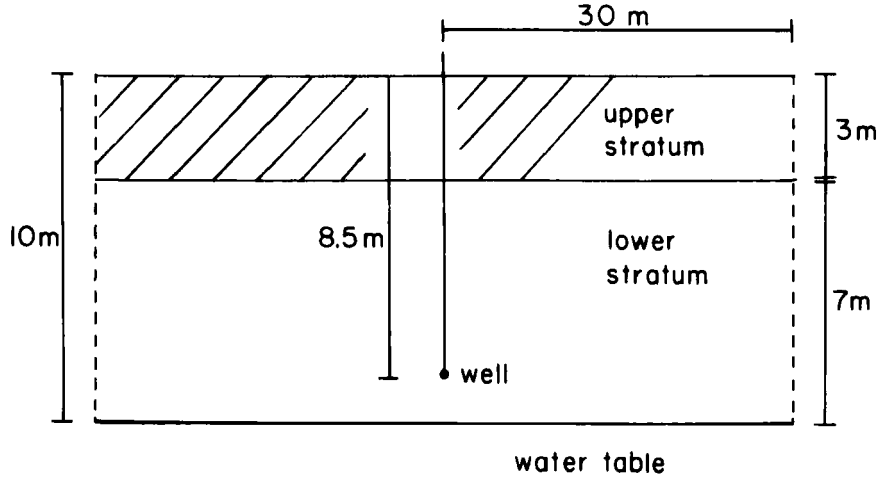


FIG. 7. The domain of interest for Runs 1 to 5.

TABLE 4
Parameters for Runs 1-5

| | |
|---|---|
| Radius of zone of influence | 30 m |
| Depth of water table | 10 m |
| Depth of vacuum well | 8.5 m |
| Screened radius of well | 0.12 m |
| Soil voids fraction | 0.2 |
| Temperature | 13°C |
| Depth of discontinuity in the permeability | 3 m |
| Well head pressure | 0.866 atm |

| Run | $Q$ (mol/s) | $K_z$ (upper)[a] | $K_r$ (upper)[a] | $K_z$ (lower)[a] | $K_r$ (lower)[a] |
|---|---|---|---|---|---|
| 1 | 0.016 | 0.1 | 0.1 | 0.01 | 0.01 |
| 2 | 0.032 | 0.1 | 0.1 | 0.02 | 0.02 |
| 3 | 0.16 | 0.1 | 0.1 | 0.1 | 0.1 |
| 4 | 0.16 | 0.02 | 0.02 | 0.1 | 0.1 |
| 5 | 0.16 | 0.01 | 0.01 | 0.1 | 0.1 |

[a]Units of the permeabilities are $m^2/atm \cdot s$.



Figure 8 shows plots of the soil vacuum (in inches of water) as a function of radial distance from the well, $r$, for piezometers at a depth of 1.5 m. The effects of the different permeability values are evident at all distances. Discrimination between Run 3 (permeability constant throughout the domain of interest) and Runs 1 and 2 (permeability smaller in the underlying layer) is greatest for small values of $r$.

Plots of soil vacuum as a function of $r$ for piezometers at a depth of 4.5 m are shown in Fig. 9. Again, the plots are such as to permit discrimination between the three cases (permeability of the overlying layer greater than, equal to, or less than the permeability of the underlying layer).

Of particular interest is the distance to which the influence of the vacuum well extends. It is apparent from both Fig. 8 and Fig. 9 that the presence of an overlying zone of low permeability, with the vacuum well screened in the more permeable region, results in a very large radius of effectiveness for the well. This has some practical significance, in that it should permit somewhat wider spacing of the vapor stripping wells, with accompanying savings.

In Fig. 10 we see plots of piezometer readings as a function of depth at a radial distance of 5.5 m from the well. It is evident that a cluster of piezometers at various depths provides an effective method for locating

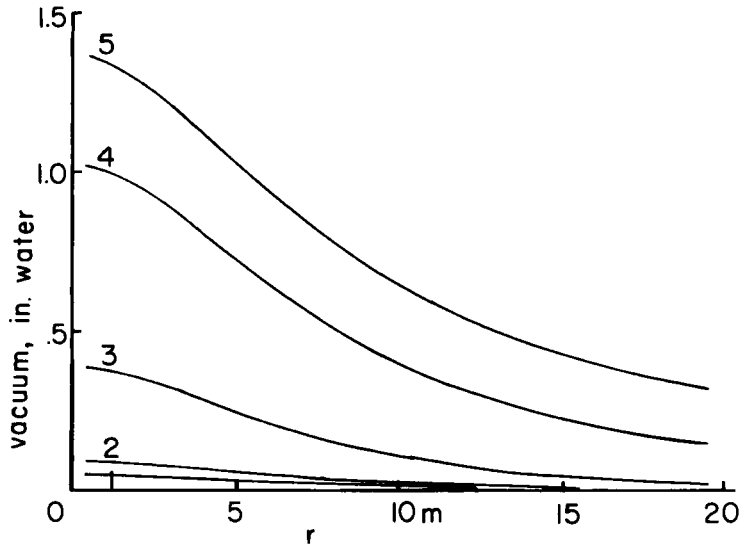


FIG. 8. Plots of soil vacuum (inches of water) versus radial distance from the vacuum well. Depth of piezometer = 1.5 m. Other parameters are given in Table 4.

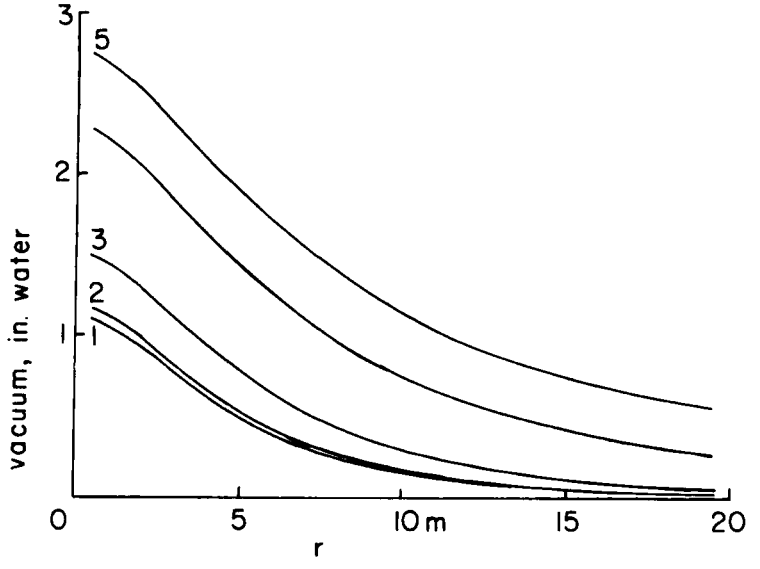


FIG. 9. Plots of soil vacuum versus radial distance from the vacuum well. Depth of piezometer = 4.5 m. Other parameters as in Table 4.

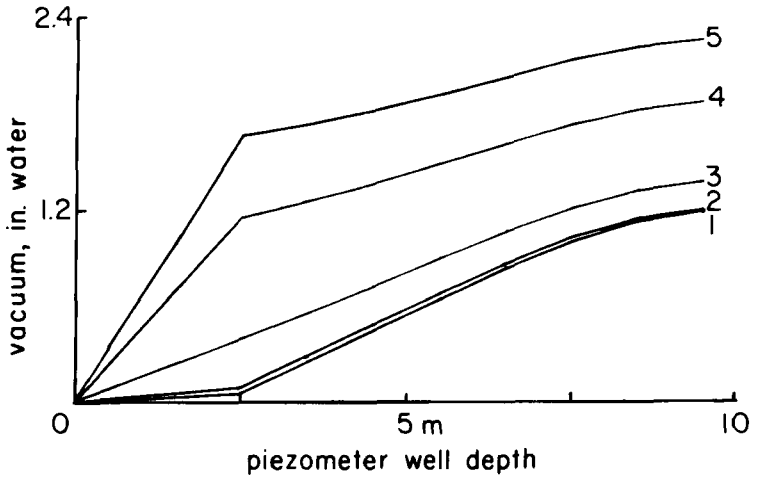


FIG. 10. Plots of soil vacuum versus piezometer depth. Radial distance from the vacuum well = 5.5 m. See Table 4 for other parameters.



variations in soil permeability with depth. The cluster should be fairly close to the vacuum well, but not so close that the soil in its vicinity has been disturbed by the drilling of the vacuum well.

The sensitivity of the piezometer readings to the permeability distribution depends markedly on the relative positions of the vacuum well, the permeability discontinuity, and the piezometer wells. For the system diagrammed in Fig. 11 (see also Table 5), the differences in the soil gas pressure distributions (see Figs. 12–14) are much less marked than those shown in Figs. 8–10 for the system diagrammed in Fig. 7. Evidently one would be well-advised to make use of well logs and test boring results in designing a vacuum well-piezometer well array for determining permeabilities with optimal sensitivity. This model should be useful in assessing the sensitivities of alternative designs. Then, when piezometer data are available, the model can be used with these and the well log and test boring data to determine the permeabilities of the various strata present.

The effect of the boundary conditions employed around the periphery of the cylindrical zone of influence depends very strongly on the ratio of the radius of the zone of influence to the depth of the vacuum well. Figure 15 show plots of soil gas vacuum versus radial distance for a well depth of

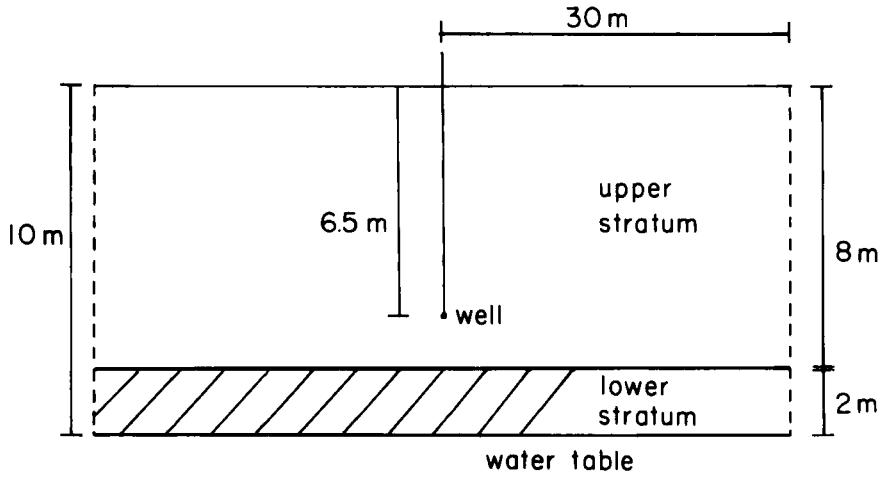


FIG. 11. The domain of interest for Runs 6 to 8.



TABLE 5
Parameters for Runs 6–8

| | |
|---|---|
| Radius of zone of influence | 30 m |
| Depth of water table | 10 m |
| Depth of vacuum well | 6.5 m |
| Screened radius of well | 0.12 m |
| Soil voids fraction | 0.2 |
| Temperature | 13°C |
| Depth of discontinuity in the permeability | 8 m |
| Well head pressure | 0.866 atm |

| Run | $Q$ (mol/s) | $K_z$ (upper)[a] | $K_r$ (upper)[a] | $K_z$ (lower)[a] | $K_r$ (lower)[a] |
|---|---|---|---|---|---|
| 6 | 0.032 | 0.02 | 0.02 | 0.1 | 0.1 |
| 7 | 0.16 | 0.1 | 0.1 | 0.1 | 0.1 |
| 8 | 0.16 | 0.1 | 0.1 | 0.02 | 0.02 |

[a]Units of the permeabilities are $m^2/atm \cdot s$.

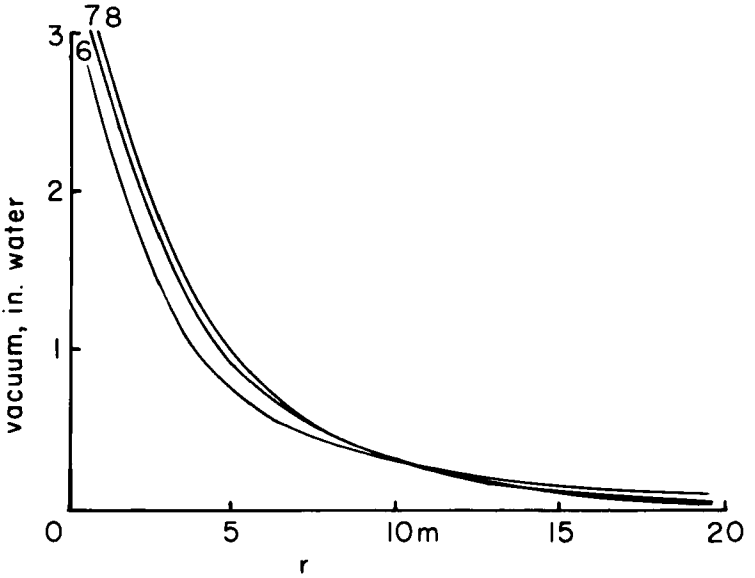


FIG. 12. Plots of soil vacuum versus radial distance from the vacuum well. Depth of piezometer = 4.5 m. Other parameters as in Table 5.

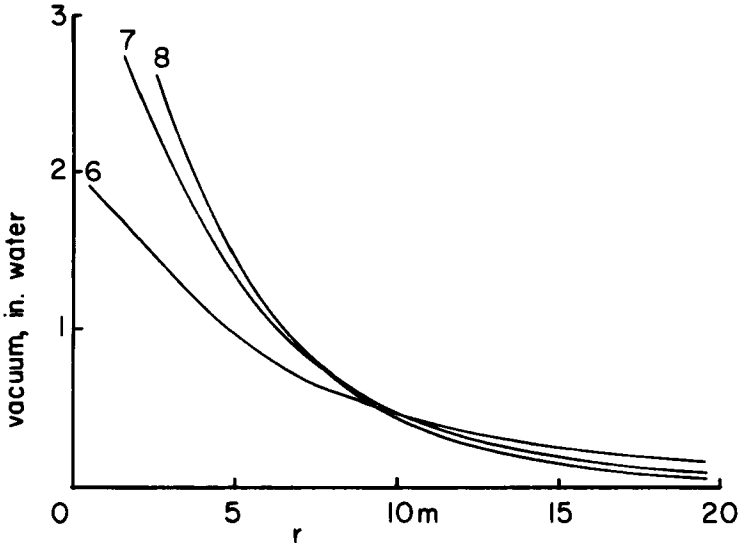


FIG. 13. Plots of soil vacuum versus radial distance from the vacuum well. Depth of piezometer = 9.5 m. Other parameters as in Table 5.

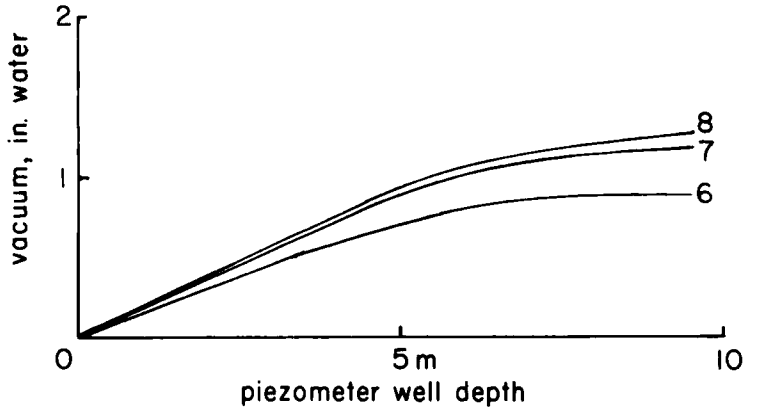


FIG. 14. Plots of soil vacuum versus piezometer depth. Radial distance from the vacuum well = 5.5 m. Other parameters are given in Table 5.



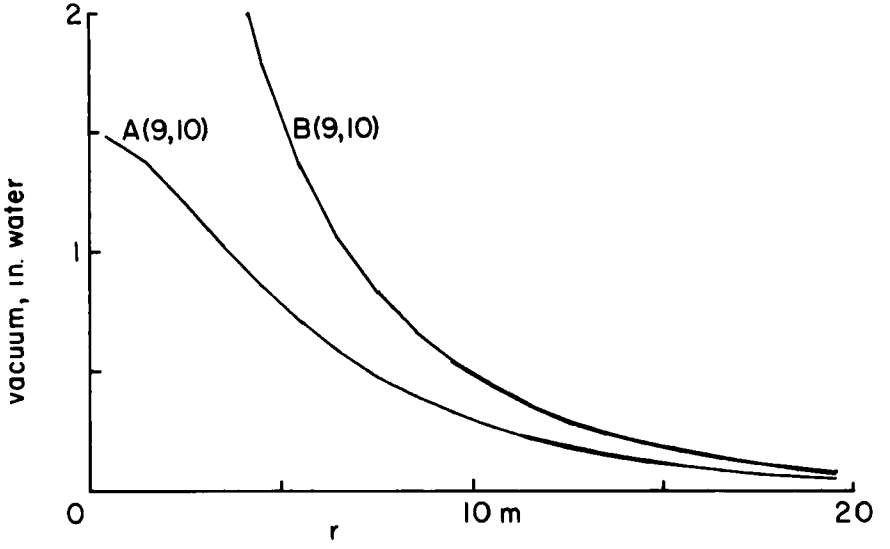


FIG. 15. Plots of soil vacuum versus radial distance. Depths of the piezometer wells are 4.5 m (Curve A) and 9.5 m (Curve B). At this scale the curves for the two boundary conditions [$P(r = 30\text{ m}) = 1$ atm and $\partial P/\partial r\ (r = 30\text{ m}) = 0$] appear identical. Parameters are given in Table 6.

TABLE 6
Parameters and Boundary Conditions for Runs 9 and 10

| | |
|---|---|
| Radius of zone of influence | 30 m |
| Depth of water table | 10 m |
| Depth of vacuum well | 8.5 m |
| Screened radius of well | 0.12 m |
| Soil voids fraction | 0.2 |
| Temperature | 13°C |
| Permeability components $K_r$ and $K_z$ | 0.1 $m^2$/atm · s |
| $Q$ | 0.16 mol/s |
| Boundary conditions: | |
| Run 9 | $\partial P/\partial r(r = 30\text{ m}) = 0$ |
| Run 10 | $P(r = 30\text{ m}) = 1$ atm |



8.5 m and a zone of influence of 30 m. The parameters and boundary conditions are given for these two runs in Table 6. The boundary conditions [$P(r = 30\text{ m}) = 1$ atm and $\partial P(r = 30\text{ m})/\partial r = 0$] yield results which appear indistinguishable both at depths of 4.5 and 9.5 m. Evidently this boundary ($r = 30$ m) is sufficiently far from the well that the influence of the type of boundary condition used on this outer surface is negligible.

On the other hand, if the well depth is 8.5 m and the radius of the zone of influence is only 10 m, the effect of the boundary condition used on the surface $r = 10$ m is very marked. Plots of soil gas vacuum versus radial distance at depths of 4.5 and 9.5 m are shown in Figs. 16 and 17, respectively (see also Table 7), and show quite substantial differences. In Fig. 18 the soil vacuum is plotted against depth at a radial distance of 4.5 m; again, the differences between the run with $\partial P(r = 10\text{ m})/\partial r = 0$ (Run 11) and that with $P(r = 10\text{ m}) = 1$ atm (Run 12) are relatively large.

We conclude on the basis of these and other runs that this boundary condition effect becomes unimportant when the radius of the zone of influence is at least three times the well depth.

One hopes that the horizontal variation of the permeability tensor is negligible over the zone of influence of a vapor stripping well. If this is not the case, then one must in general use a full-fledged three-dimensional model. Such a model would be too large to run on microcomputers such as the IBM PC-AT and its clones, which are quite capable of handling our axially symmetric model.

Once the permeability has been mapped out, one can then calculate gas velocity fields for a vapor stripping well from Darcy's law,

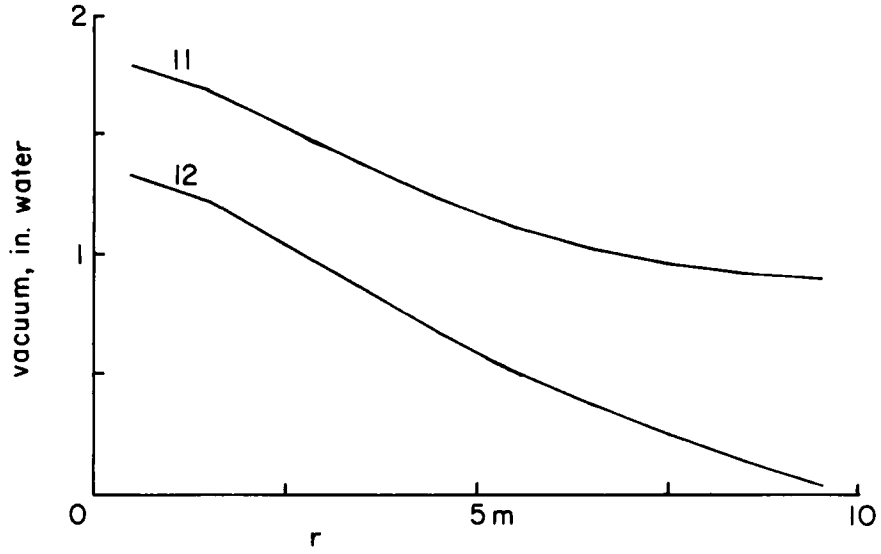


FIG. 16. Plots of soil vacuum radial distance from the vacuum well. $\partial P/\partial r(r = 10\text{ m}) = 0$ for Run 11; $P(r = 10\text{ m}) = 1$ atm for Run 12. Piezometer well depth = 4.5 m. See Table 7 for parameters.

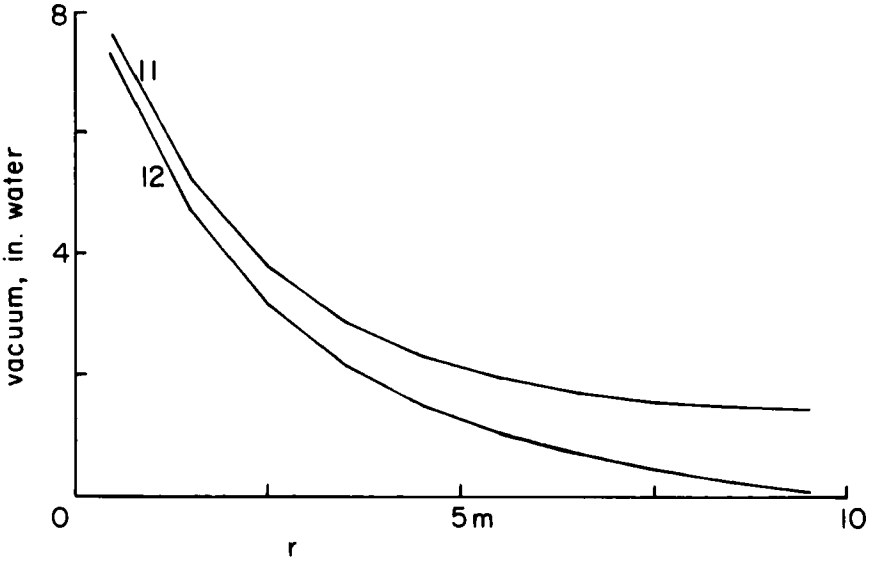


FIG. 17. Plots of soil vacuum versus radial distance from the vacuum well, Runs 11 and 12. Piezometer well depth = 9.5 m. See Table 7 for parameters.

TABLE 7
Parameters and Boundary Conditions for Runs 11 and 12

| | |
|---|---|
| Radius of zone of influence | 10 m |
| Depth of water table | 10 m |
| Depth of vacuum well | 8.5 m |
| Screened radius of well | 0.12 m |
| Soil voids fraction | 0.2 |
| Temperature | 13°C |
| Permeability components $K_r$ and $K_z$ | 0.1 $m^2/atm \cdot s$ |
| $Q$ | 0.16 mol/s |
| Boundary conditions· | |
| Run 11 | $\partial P/\partial r(r = 30\ m) = 0$ |
| Run 12 | $P(r = 30\ m) = 1$ atm |



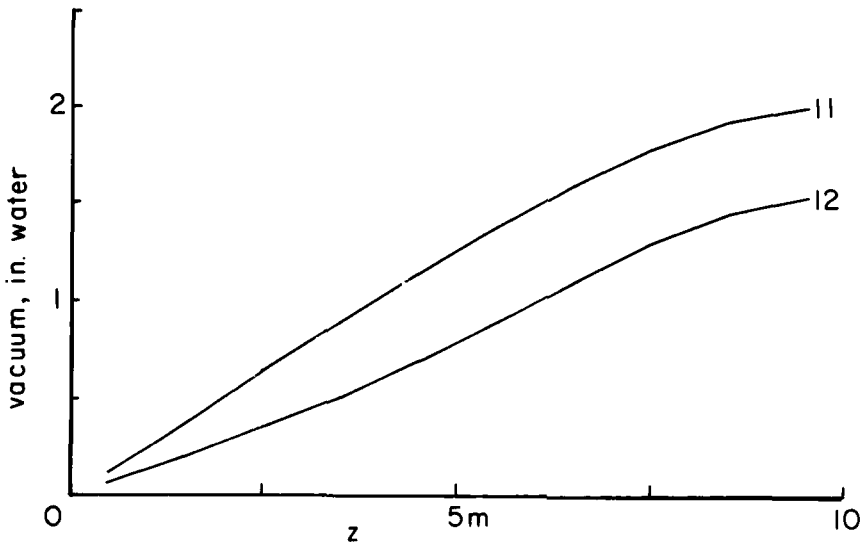


FIG. 18. Plots of soil vacuum versus piezometer depth. Radial distance = 4.5 m. $\partial P/\partial r$ ($r$ = 10 m) for Run 11; $P(r = 10\ m) = 1$ atm for Run 12. See Table 7 for parameters.

$$v = -\mathbf{K}\nabla P \tag{49}$$

$$v_r = -\mathbf{K}_r \partial P/\partial r \tag{50}$$

$$v_z = -\mathbf{K}_z \partial P/\partial z \tag{51}$$

These can then be used in the model for soil vapor stripping which was presented earlier (2–4).

## CONCLUSIONS

Our vapor stripping model has been extended to media having anisotropic and variable permeabilities. Piezometric measurements of soil gas pressures around a vacuum well, plus test boring and well log data, provide a means for approximating the permeability tensor function. This work should substantially increase the utility of the vapor stripping model.



### Acknowledgment

D.J.W. is obliged to the Water Resources Research Center of the University of Tennessee for a grant in support of this work.

### REFERENCES

1. F. Schwille, *Dense Chlorinated Solvents in Porous and Fractured Media* (J. F. Pankow, translator), Lewis Publishers, Chelsea, Michigan 1988.
2. D. J. Wilson, A. N. Clarke, and J. H. Clarke, *Sep. Sci. Technol., 23,* 991 (1988).
3. K. Gannon, D. J. Wilson, A. N. Clarke, R. D. Mutch Jr., and J. H. Clarke, *Ibid., 24,* 831 (1989).
4. D. J. Wilson, A. N. Clarke, and R. D. Mutch Jr., *Ibid., 24,* 939 (1989).
5. W. L. Wootan Jr. and T. Voynick, *Forced Venting to Remove Gasoline Vapor from a Large-Scale Aquifer,* Submitted by Texas Research Institute to American Petroleum Institute, Washington, D.C., January 13, 1984. See also Texas Research Institute, Inc., *Examination of Venting for Removal of Gasoline Vapors from Contaminated Soil,* Submitted to American Petroleum Institute, API Publication 4429, 1980.
6. A. N. Clarke, "Zone I Soil Decontamination through in Situ Vapor Stripping Processes," Contract 68-02-4446, Final Report to FPA, AWARE, Inc., April 1987.
7. Woodward-Clyde Consultants, "Performance Evaluation Pilot Scale Installation and Operation, Soil Gas Vapor Extraction System, Time Oil Company Site, Tacoma, Washington, South Tacoma Channel, Well 12A Project," Work Assignment 74-ON14.1, Walnut Creek, California, December 13, 1985.

8. G. J. Anastos, P. J. Parks, M. H. Corbin, and M. F. Coia, "In Situ Air Stripping of Soils Pilot Study," Submitted by Roy F. Weston, Inc., to U.S. Army Toxic and Hazardous Materials Agency, Aberdeen Proving Ground, Maryland, Report AMXTH-TE-TR-85026, October 1985.
9. W. L. Crow, E. P. Anderson, and E. Minugh, *Subsurface Venting of Hydrocarbon Vapors from an Undergound Aquifer,* Submitted by Riedel Environmental Services Co. and Radian Corp. to American Petroleum Institute, Washington, D.C., API Publication 4410.
10. R. E. Bailey and D. Gervin, "In Situ Vapor Stripping of Contaminated Soils: A Pilot Study," in *Proc., 1st Annu. Hazardous Materials Management Conf./Central,* 1988, p. 207.
11. H. J. Lord, "Activated Carbon Treatment of Contaminants from a Soil Venting Operation: A Case Study," in *Proc., 1st Annu. Hazardous Materials Management Conf./Central,* title only, Liberty Environmental Systems, Inc., 1988.
12. P. A. Michaels, "Technology Evaluation Report: Site Program Demonstration Test, Terra Vac In-Situ Vacuum Extraction System, Groveland, Massachusetts," Enviresponse, Inc., Livingston, New Jersey, EPA Contract 68-03-3255, 1989.
13. A. N. Clarke and D. J. Wilson,"A Phased Approach to the Development of In Situ Vapor Stripping Treatment," *Proc., 1st Annu. Hazardous Materials Management Conf./Central,* 1988, p. 191.
14. D. J. Wilson, "Mathematical Modeling of In Situ Vapor Stripping of Contaminated Soils" in *Proc., 1st Annu. Hazardous Materials Management Conf./Central,* 1988, p. 94.
15. R. A. Freeze and J. A. Cherry, *Groundwater,* Prentice-Hall, Englewood Cliffs, New Jersey, 1979, pp. 32–36.
16. W. R. Smythe, *Static and Dynamic Electricity,* 2nd ed., McGraw-Hill, New York, 1950.
17. H. B. Dwight, *Tables of Integrals and Other Mathematical Data,* Macmillan, New York, 1949, Eq. 200.03, p. 45.
18. F. S. Shaw, *Relaxation Methods,* Dover, New York, 1953.


*Received by editor May 19, 1989*